Available online at www.sciencedirect.com
ScienceDirect
International Journal of Thermal Sciences 48 (2009) 881–890
International Journal of Thermal Sciences
www.elsevier.com/locate/ijts

Optimal configuration of discrete heat sources in a vertical duct under conjugate mixed convection using artificial neural networks

T.V.V. Sudhakar, C. Balaji *, S.P. Venkateshan

Heat Transfer and Thermal Power Laboratory, Department of Mechanical Engineering, Indian Institute of Technology, Madras, Chennai 600 036, India

Received 29 January 2008; received in revised form 1 May 2008; accepted 19 June 2008

Available online 30 July 2008

Abstract

This paper reports the results of a numerical investigation of the problem of finding the optimum configuration for five discrete heat sources, mounted on a wall of a three-dimensional vertical duct under mixed convection heat transfer, using artificial neural networks (ANN). The objective is to locate the positions for the five heat sources in such a way that the maximum temperature of any of the heat sources in a given configuration is a minimum. The three-dimensional governing equations of mass, momentum and energy equations for the fluid flow and the energy equation for the solid regime have been solved by using FLUENT 6.3 and a database of temperature versus configuration was generated. The temperature database developed from CFD simulations is used to train the neural network. The trained neural network predicts the temperature of the heat sources very accurately and much faster than the CFD software. With the use of this network, an exhaustive search for all possible configurations was done that resulted in a global optimum for the problem.
© 2008 Elsevier Masson SAS. All rights reserved.

Keywords: Conjugate mixed convection; Artificial neural networks; Protruding heat sources; Optimization

1. Introduction

Computational Fluid Dynamics (CFD) simulations are typically time consuming for complex problems and many a time are not cost effective. Many situations in practice require a large number of CFD computations for making engineering judgment. The problem of placing electronic components on a substrate is one such problem, wherein the reliability of the components depends upon the maximum temperature during operation. The relative positions of the components influence the flow and consequently affect their temperatures. In general, the selection of the best possible configuration out of several thousand possibilities is not trivial. The solution for each configuration can be obtained by solving simultaneously the governing equations of continuity, momentum and energy equations for the flow and additional energy equation for the solid, if wall conduction is considered. In recent years, artificial neural network (ANN) has been increasingly utilized in science and engineering, as it has a remarkable ability of self-learning and self-organization. A neural network can employ previously acquired knowledge to respond to new information rapidly and automatically. The position of the components on board is an important area of current research in electronic cooling. Da Silva et al. [1–3] addressed the problems of allocation of in line heating elements mounted on the wall/vertical open channels cooled by forced/free convection and showed, analytically, using constructal theory, that the heat sources must be distributed non-uniformly in both the forced and free convection regimes. Furthermore, they reported that the spacing between the heat sources depends on the flow parameters. Dias and Milanez [4] studied the optimization of natural convection heat transfer for two-dimensional flush mounted heat source(s) in a cavity using Genetic Algorithms. Liu and Phan-Thien [5] studied the problem of optimum spacing of three heated chips mounted on a conductive substrate in an enclosure and concluded that the centre-to-centre distances between the chips follow a geometric series with a common ratio 1.168. Chen and Liu [6] investigated, experimentally, the problem of forced convection in a parallel plate channel with nine modules mounted on a printed circuit board and determined the optimum spacing

* Corresponding author. Fax: +91 044 2257 0509.
E-mail address: balaji@iitm.ac.in (C. Balaji).

1290-0729/$ – see front matter © 2008 Elsevier Masson SAS. All rights reserved.
doi:10.1016/j.ijthermalsci.2008.06.013

Nomenclature

A_{wetted}	wetted area of the heat source	m^2
C_p	specific heat	J/kg K
Gr^*	modified Grashof number, $g\beta\Delta T_{\text{ref}}h^3/\nu^2$	
h	height of the heat source	m
$\overline{h}$	average heat transfer coefficient	W/m^2 K
H	height of the duct	m
k	thermal conductivity	W/m K
lr	learning rate	
Nu	average Nusselt number, $\overline{h}S/k$	
p	pressure	N/m^2
Q	heat transfer rate	W
Q_{gen}	volumetric heat generation	W/m^3
Re	Reynolds number based on S, $V_\infty S/\nu$	
S	spacing between the walls of the channel	m
t	heat source thickness	mm
T	temperature	°C
U	velocity in the X-direction	m/s
V	velocity in the Y-direction or volume of the heat source as the case may be	m/s or m^3
$\mathbf{V}$	velocity vector	m/s
W	velocity in the Z-direction	m/s
x, y, z	coordinate directions	m
X, Y	position coordinates of the heat sources	m

Greek symbols

ΔT	$(T - T_\infty)$	°C
ΔT_{ref}	reference temperature difference $Q_{\text{gen}}Vh/A_{\text{wetted}}k_f$	
α	thermal diffusivity of the fluid, $k/\rho C_p$,	m^2/s
β	isobaric cubic expansivity of the fluid	1/K
θ	non-dimensional temperature of the heat source, $(T - T_\infty)/(T_{\max} - T_\infty)$	
μ	momentum parameter in the ANN	
ν	kinematic viscosity of fluid	m^2/s
ρ	density	kg/m^3

Subscripts

dec	decrement
f	fluid
h	heat source
inc	increment
max	maximum
m	mean value
ref	reference
s	solid
∞	ambient/inlet

ratio. Queipo et al. [7] demonstrated an adaptive search methodology, based on Genetic Algorithms, for the optimal configuration of heated modules of different sizes in a channel under forced convection. Rajeev Reddy and Balaji [8] used artificial neural networks coupled with micro genetic algorithm to locate three heat sources optimally in a ventilated cavity under forced turbulent convection. Sablani et al. [9] used ANN to predict the heat transfer coefficient at the surface from the measurement of the temperature–time history inside a solid body for the two geometries, namely a cube and a semi-infinite plate. Mahmoud et al. [10] designed three types of neural networks for predicting flow variables in a partitioned enclosure. Thibault and Grandjean [11] introduced neural networks in the field of heat transfer for data analysis. Gregory et al. [12] used artificial neural networks to correlate experimentally determined Colburn j-factors and Fanning friction factors for flow of liquid water in straight tubes with helical fins. Islamoglu and Kurt [13] developed an ANN model to estimate Nusselt numbers for air flowing in corrugated channels.

The literature review presented above shows that very few investigations have been reported on the application of artificial neural networks in the area of fluid flow and heat transfer problems in general. For complex three-dimensional problems, ANN may have the potential to bring out more information on quantities of interest like Nusselt number or maximum temperature, based on a limited parametric study. Thus ANN can serve as a "fast" forward problem in the parlance of optimization. With the "fast" model in place, one can afford the luxury of an exhaustive search in the determination of the optima in certain problems. With this objective in mind, the present work explores the possibility of using a trained network to predict the temperatures of discrete heat sources for different configurations (the position of discrete heat sources), by using a few CFD simulations and finally arrives at the best possible configuration by an exhaustive search in the solution space.

2. Problem description

Three-dimensional conjugate mixed convection in a vertical duct with a very low aspect ratio (S/W) normal to the flow direction has been considered, with five identical finite heat sources, each generating heat at a uniform rate, placed at arbitrary positions in a regular grid. The schematic of the geometry considered for investigation is shown in Fig. 1, along with the geometric details in the problem domain. Since the ratio of the dimensions of the heat source and the wall in the transverse direction is small, the flow around the heat source can significantly influence the heat transfer characteristics. For simplicity, 25 uniformly spaced positions for the heat sources are taken at the centre of the left wall which can be treated as a substrate as shown in Fig. 2. The configuration shown in Fig. 2 is denoted as 54-41-43-45-32. Each position of the heat source is represented by a number ij where i and j are the corresponding row and column numbers, as used in conventional matrix algebra to denote the elements of a matrix. In each row, a heat source can be placed in any of the 5 places. A large number of configurations of five heat sources are possible in a 5×5 layout. In practice, there could be several such components that need to be placed in a given area on the substrate, keeping the maximum and average temperature of the components within the prescribed limits.

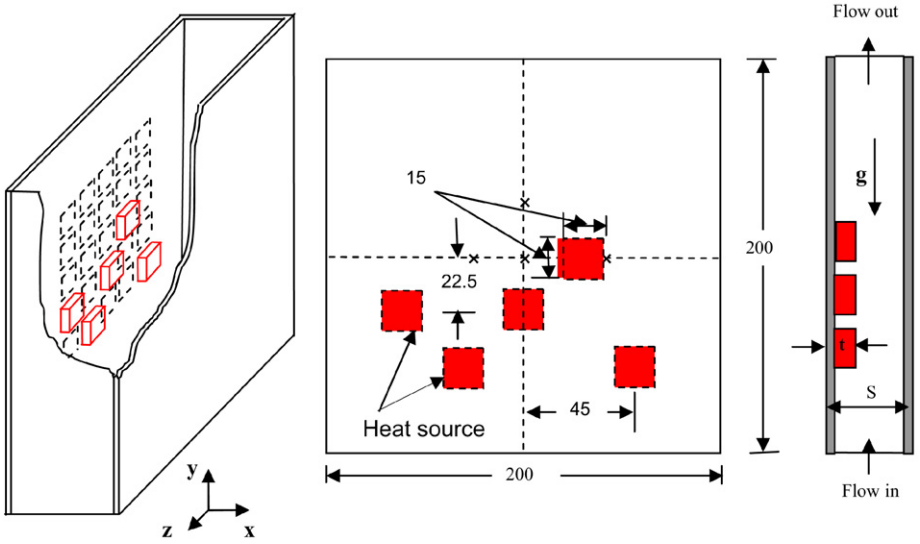

Fig. 1. Physical situation considered for the position of optimization of five identical heat sources.

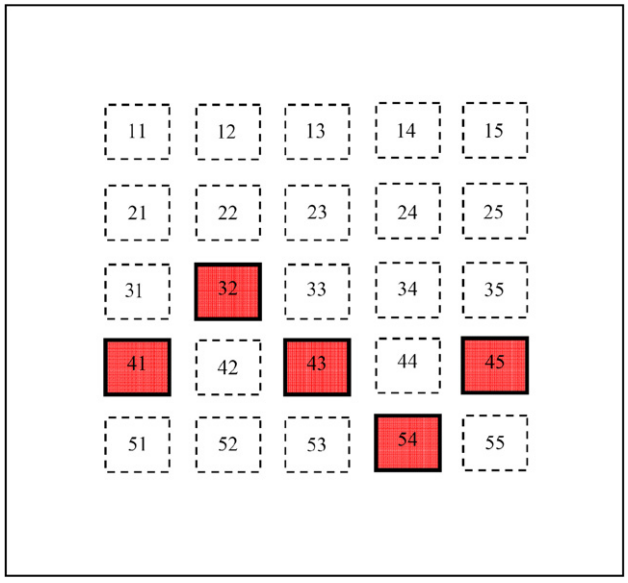

Fig. 2. Representation of position of heat sources on the substrate.

Table 1
Thermo physical properties of the heat source and the substrate

Material	Heat source	Substrate
Density (kg/m^3)	2800	1162
Specific heat (J/kg K)	950	1466
Thermal conductivity (W/m K)	3.5	0.2

The thermo-physical properties of the heat source and duct are given in Table 1.

2.1. Governing equations

The medium under consideration is air. The flow is considered to be steady, incompressible and laminar, with constant fluid properties except for density. The density changes are modeled with the use of the Boussinesq approximation. Radiation heat transfer, viscous heat dissipation, compressibility effects and contact resistance between the heat source and the substrate are considered to be negligible. To account for conjugate convection, the energy equation is solved for the solid domain as well. It is assumed that no temperature jump occurs at the solid–solid interface. Based on the above assumptions, the governing equations for mass, momentum and energy for a steady three-dimensional flow in the fluid domain and the energy equation in the solid region are as follows.

Fluid:
Continuity equation

$$\nabla.\mathbf{V} = 0 \tag{1}$$

Momentum equation

$$(\mathbf{V}.\nabla)\mathbf{V} = -\frac{\nabla p}{\rho} + \nabla^2\mathbf{V} + \mathbf{g}(T - T_\infty) \tag{2}$$

Energy equation

$$(\mathbf{V}.\nabla)T = \alpha\nabla^2 T \tag{3}$$

Solid:
Energy equation

$$\nabla^2 T + \frac{Q_{\text{gen}}}{k_s} = 0 \tag{4}$$

2.2. Boundary conditions

No slip condition as given in Eq. (5) are applied to all fluid–solid surface interfaces

$$U = V = W = 0 \tag{5}$$

and the solid surfaces other than fluid–solid interfaces are assumed to be adiabatic

$$\frac{\partial T}{\partial n} = 0 \tag{6}$$

At the outlet, the out flow condition which corresponds to zero diffusion for all flow variables is imposed. Since the height to

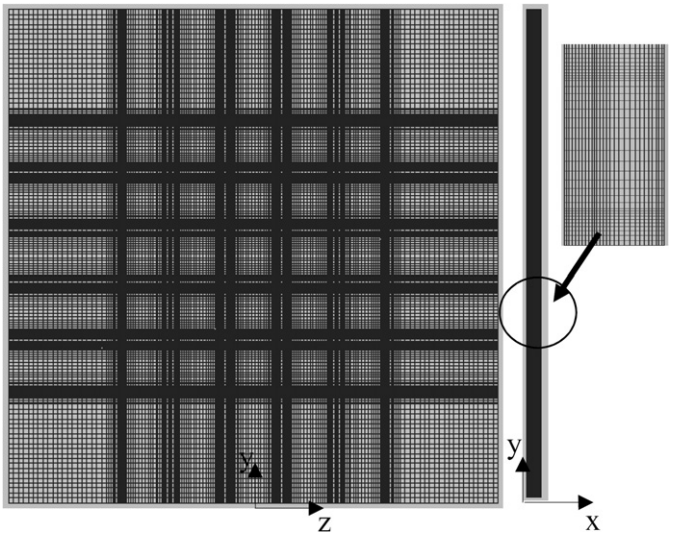

Fig. 3. A typical non-uniform structured grid used in the present study.

spacing of the channel is high, the error associated with this boundary condition is small.

At the inlet the flow is one-dimensional, with a uniform velocity of V_∞ and a uniform temperature of T_∞ and this translates to the following boundary conditions.

$$U = W = 0 \tag{7}$$

$$V = V_\infty \tag{8}$$

$$T = T_\infty \tag{9}$$

2.3. Grid independence study

A non-uniform and structured grid is considered for solving the problems under investigation. A fine mesh is generated using GAMBIT 2.2 around the solid chip surface with a minimum cell size of 10 μm and with a successive ratio of 1.1 and 1.2 in the span-wise and transverse directions, respectively. The details of the grid dependence test for a typical case are given in Table 2. Since the present study considers five heat sources of different configurations, a common grid pattern shown in Fig. 3 has been made use of. This common grid pattern saves a lot of time in meshing for different configurations on one hand, while on the other it increases the computational time where fewer nodes would suffice for some configurations. Even so, it is observed that the overall time for both meshing and computations is greatly reduced by the use of this strategy. The maximum difference in the temperature between a grid pattern with 0.5 million nodes and that with 1.44 million nodes is found to be less than 1 °C and all subsequent calculations have been done with the grid having 0.5 million nodes.

2.4. Numerical scheme

Eqs. (1)–(4) together with the boundary conditions shown in Eqs. (5)–(9) form a set of coupled non-linear partial differential equations and have been solved using FLUENT 6.3. The numerical scheme adopted is a segregated solver with implicit

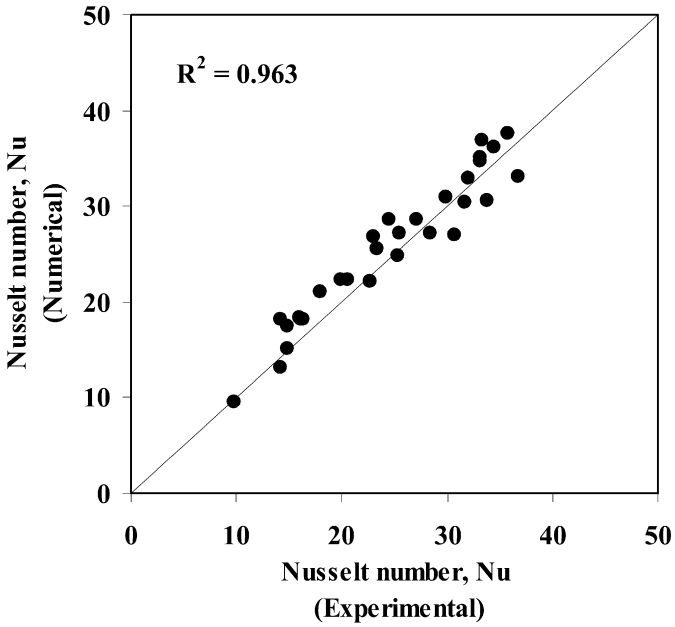

Fig. 4. Parity plot showing the Nusselt number estimated by the experiments (Alex et al. [14]) and the present numerical simulations.

formulation. The pressure and velocity equations are linked by the SIMPLE algorithm. A residual of 10^{-6} for the equations of continuity, and momentum and 1×10^{-12} for the energy equation have been employed as the convergence criteria. The overall energy and mass balance were found to be observed within 0.05% upon convergence. Since the present study focuses on geometric optimization, all calculations were done for $Re = 490$ and $Gr^* = 2.4 \times 10^4$.

2.5. Validation of the numerical scheme

The present numerical scheme is validated with the experimental data of Alex et al. [14] for a single heat source mounted on one of the walls of a channel. The study covered both natural convection and forced convection regimes over a wide range of Grashof numbers ($4 \times 10^4 \leqslant Gr \leqslant 12 \times 10^4$) and Reynolds numbers ($0 \leqslant Re \leqslant 1250$) respectively in the laminar regime. The experiments were conducted with various sizes of the heated modules, for different values of the channel spacing. Different surface coatings were also used to study the effect of radiation properties on heat transfer. The correlation proposed in [14] for the Nusselt number for channel flow with a heated module is used to validate the numerical simulations. The physical dimensions of the geometry considered in the numerical simulations correspond to those used by the Alex et al. [14]. Fig. 4 shows a parity plot that highlights the agreement between results of the numerical simulations and the experiments. The maximum deviation between the numerical simulations and the experiments is about 14%.

3. Artificial neural networks

Neural networks use a set of processing elements loosely analogous to neurons in the brain (hence the name, neural net-

Table 2
Results of the grid independence test for $Re = 490$, $Gr^* = 2.4 \times 10^4$

Number of nodes	Temperature (°C)					Maximum percentage deviation with respect to the previous grid
	T_1	T_2	T_3	T_4	T_5	
249984	88.5	88.2	88.5	88.9	88.9	–
513024	100.0	99.7	100.0	100.4	100.4	13
1441188	99.4	98.9	99.4	100.1	100.1	0.8

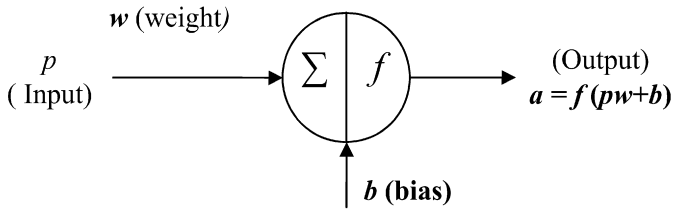

Fig. 5. A basic neuron structure.

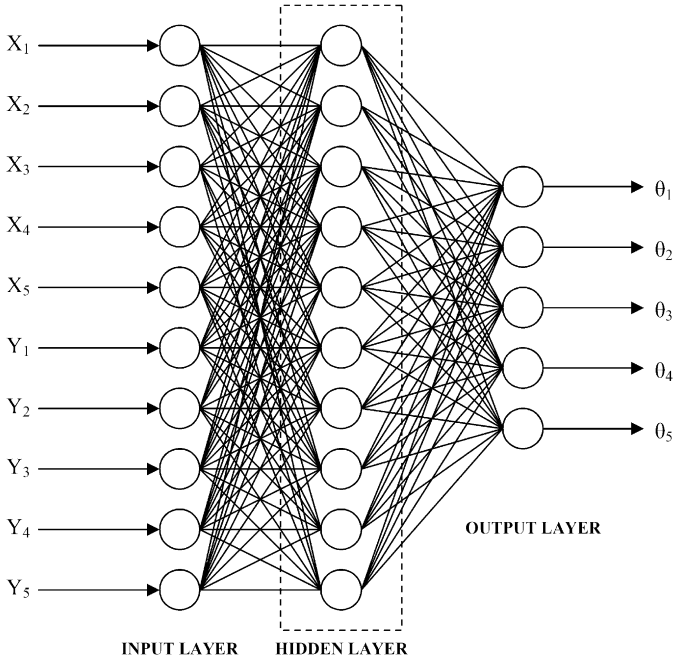

Fig. 6. Schematic of the neural network architecture employed for this study.

works). These nodes are interconnected in a network that can then identify patterns in data as they get exposed to the data. In a sense, the network learns from experience just as we do. This distinguishes neural networks from traditional computing programs that simply follow instructions in a fixed sequential order. One of the most important features of a neural network is its flexibility and ability to learn complicated relationships based on the data. Fig. 5 shows the basic structure of a neuron which performs a non-linear transformation of the weighted sum of the inputs to produce an output. A neural network consists of one input layer; one or more hidden layer(s) and one output layer with a large number of inter connected neurons. For the present investigation, a back propagation feed forward neural network or multi layer perceptron (MLP) shown in Fig. 6 has been considered. Back propagation is the most widely used learning process in neural networks today.

The Levenberg–Marquardt back propagation algorithm that represents a simplified version of Newton's method is applied as the training algorithm in this study. Newton's method is a well-established numerical optimization technique with a quadratic rate of convergence. As the input and output data are normalized between 0 and 1, the log sigmoid function is used as the activation function for all the hidden layer neurons and the output layer. Since there are ten inputs, i.e. two coordinates (X_i, Y_i) for each position of the heat source to the neural network, the network has ten neurons in the input layer and five neurons in the output layer with each neuron corresponding to the temperature (θ_i) of respective heat source. There are no established methods to determine the number of hidden layers or the neurons in each hidden layer, and so they have been determined in this study by an iterative procedure. When there are too few neurons in the hidden layer, the performance of the network is not satisfactory. However, if there are too many, convergence is very slow and may even be compromised by local minima. The optimal number of hidden neurons is determined empirically, as the minimal number of neurons for which the prediction performance is sufficient without leading to over fitting or an unreasonably long computational time. The use of the mean squared error (MSE) is an excellent criterion for evaluating the performance of the neural network. The back propagation algorithm uses iterative steepest descent gradient algorithm to minimize the mean squared error by adjusting the weights suitably. Several neural networks with different architectures were tried to finally arrive at a three layer network (including the input layer) with 10 neurons in the hidden layer. A few of the several network architectures with their maximum performance (correlation coefficient R^2 is above 0.9) are given in Table 3, which were obtained after repeated initializations of each of the network configurations. The performance parameters used in the present network are given in Table 4. The optimum performance parameters for the network are obtained iteratively by changing the number of neurons in the hidden layer or allowing a change in the parameters like momentum rate, learning rate as shown in Table 4. The learning rate (lr) parameter specifies the magnitude of the update step for the weights in the negative gradient direction. If the learning rate is too small, the learning algorithm will modify the weights sluggishly and a relatively large number of iterations will be required for convergence. Too large learning rate leads to a possible divergence. The momentum parameter tends to aid the convergence. In order to decide the architecture of the neural network, a code was written in MATLAB 7.0. For a fuller discussion on the back propagation feed forward algorithm and different performance parameters used in the training phase of the network see [15].

Table 3
Performance of the different network architectures

S. no	Number of neurons in the hidden layer 1	Number of neurons in the hidden layer 2	R^2-value (correlation coefficient)	
			Training	Testing
1	6	0	0.9943	0.9471
2	8	0	0.9939	0.9179
3	10	0	0.997	0.9926
4	12	0	0.9988	0.9471
5	14	40	0.9935	0.8435
6	16	30	0.9935	0.9219
7	18	26	0.9969	0.7948
8	20	34	0.9987	0.8298

Table 4
Performance parameters used for the learning process considered in the present study

Parameters	Value
Performance function (MRE)	10^{-6}
Momentum reduction	1
Minimum gradient	10^{-10}
μ, μ_dec, μ_inc, μ_max	0.002, 0.02, 10, 10^{10}
Learning rate	1.54

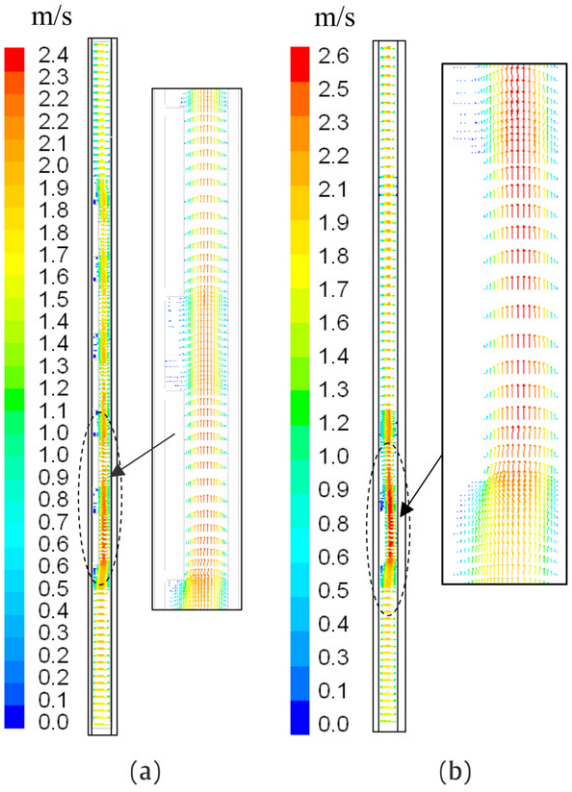

Fig. 7. Velocity contours in the span-wise direction at the mid-plane of the heat sources, (case (a)) heat sources arranged in a column, (case (b)) heat sources arranged in a row.

4. Results and discussion

In vertical ducts, the effect of buoyancy on the flow and heat transfer is expected to be significant, particularly in the laminar regime. Buoyancy induced by heating the fluid enhances the fluid motion thereby enhancing the heat transfer rate. The laminar flow field in the span-wise (x-direction) direction at the mid-plane of the heat sources is shown in Fig. 7(a), for the arrangement where the five heat sources are placed back to back in a column which is referred to as case (a) and in Fig. 7(b), for the arrangement where the five heat sources are placed side by side in a row which is referred to as case (b). From these figures, it can be seen that the flow changes from a uniform profile at the inlet to fully developed condition as it approaches the first heat source itself. The flow then gets diverted by the first heat source as it is projected on to the main flow. The flow proceeds downstream without much disturbance due to the other heat sources. This is due to the main flow plus the secondary flow that begins from the bottom and top surface of every heat source by natural convection. It can be seen further from Fig. 7, that the flow again becomes fully developed, i.e. the velocity variation in the span-wise direction is unaffected, as the flow approaches the exit. The maximum velocity for case (b) (2.6 m/s) is higher that for case (a) (2.4 m/s), suggestive of increased cooling in case (b).

The isotherms in the span-wise and transverse directions at the mid planes of the heat sources for both the cases discussed are shown in Fig. 8 (a) and (b). For case (a), the temperatures of the fluid and the heat sources increase in the direction of main flow and reach a maximum near the last heat source. The maximum temperature of the heat sources is more or less uniform in the case of five heat sources arranged in a row (case (b)), as there is little lateral thermal interaction among the heat sources. The temperatures also approach the ambient rather sharply, as one moves away from the heat sources in both the span-wise and transverse directions. The temperature distribution within the heat source is not uniform and the size of the hot spot and its location change with the position of the heat source. The area weighted average maximum temperatures of both these configurations are 165 °C and about 90 °C, respectively. Hence, the location of heat sources has a profound effect on the maximum temperatures and the problem becomes a fit case for optimization.

One of the major objectives of the present study is to explore the use of artificial neural networks to avoid the time consuming CFD simulations. A total of 127 CFD simulations were first carried out for predicting the temperature of the heat sources. These configurations were carefully chosen such that the min-

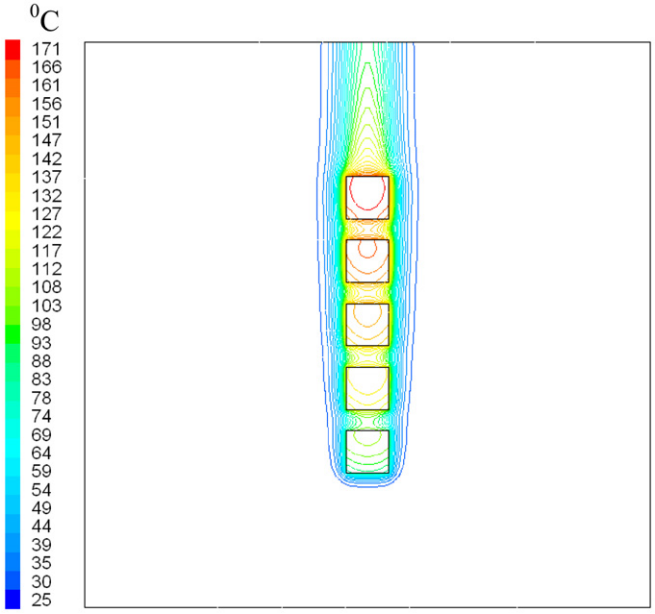

(a)

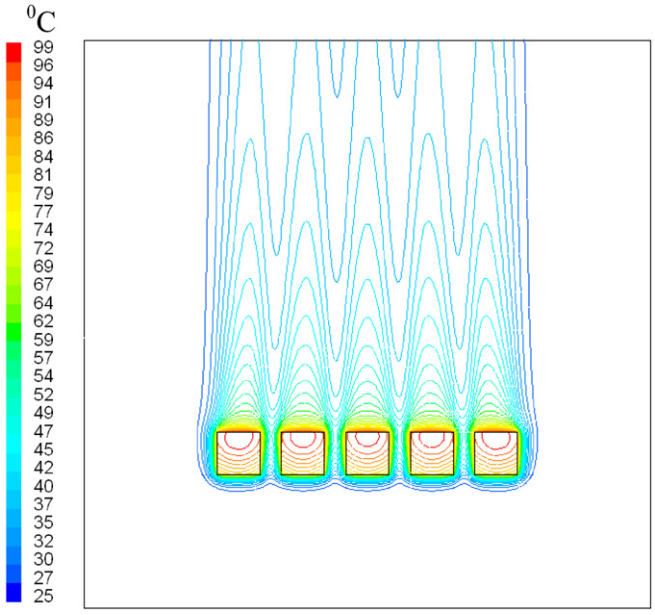

(b)

Fig. 8. Isotherms in the transverse directions in the respective mid-planes of the heat sources, (case (a)) heat sources arranged in a column, (case (b)) heat sources arranged in a row.

imum and the maximum of both X and Y coordinates were covered. Keeping this in mind, the configurations are chosen at random in the problem domain for the preparation of the data base for the purpose of training and testing the neural network. The ANN used 80% of the data base for its training and the remaining 20% of the data used for testing. The performance of the trained network is shown in Fig. 9, where the agreement between the data produced by the network and the data obtained from the numerical simulations can be clearly seen.

Fig. 10 presents a comparison of temperatures of the heat sources predicted by the neural network and temperatures di-

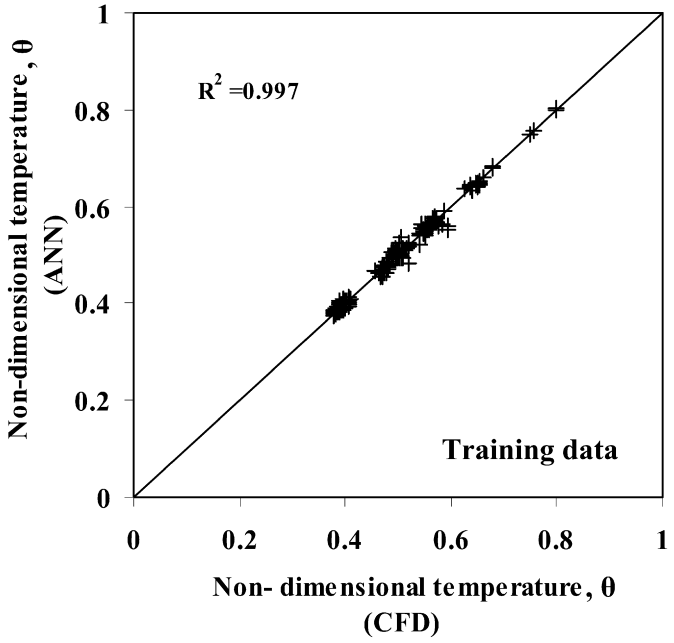

Fig. 9. Parity plot showing agreement between non-dimensional temperature (CFD simulations) and non-dimensional temperature (ANN).

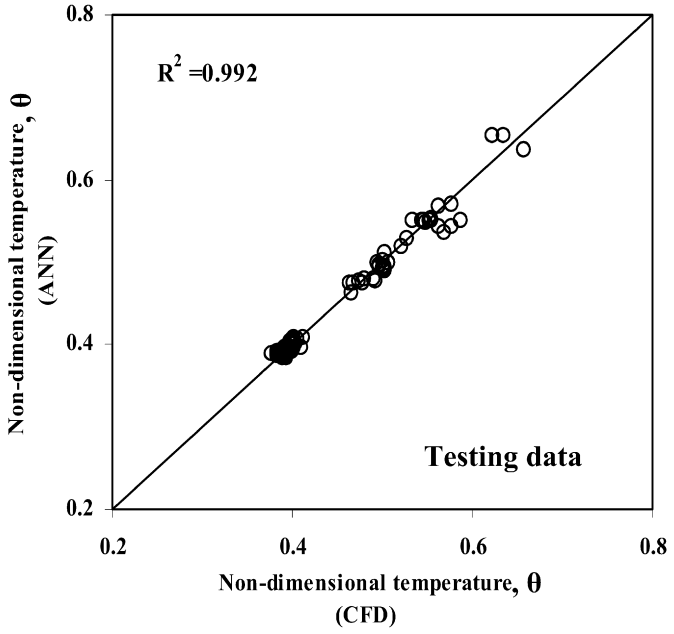

Fig. 10. Parity showing agreement between non-dimensional temperature (CFD) and non-dimensional temperature (ANN).

rectly available from the numerical simulations for cases where the data from "full" CFD solutions were not used to train the network. From the figure, it is seen that there is a good agreement between the temperatures predicted by the neural network and the actual values. The maximum temperature plays a very important role in the selection of the best configuration for the heat sources and it is imperative that the neural network predict these temperatures accurately. Fig. 11 shows the different configurations of the heat sources whose temperature data is fed to the trained network, the corresponding output is converted into

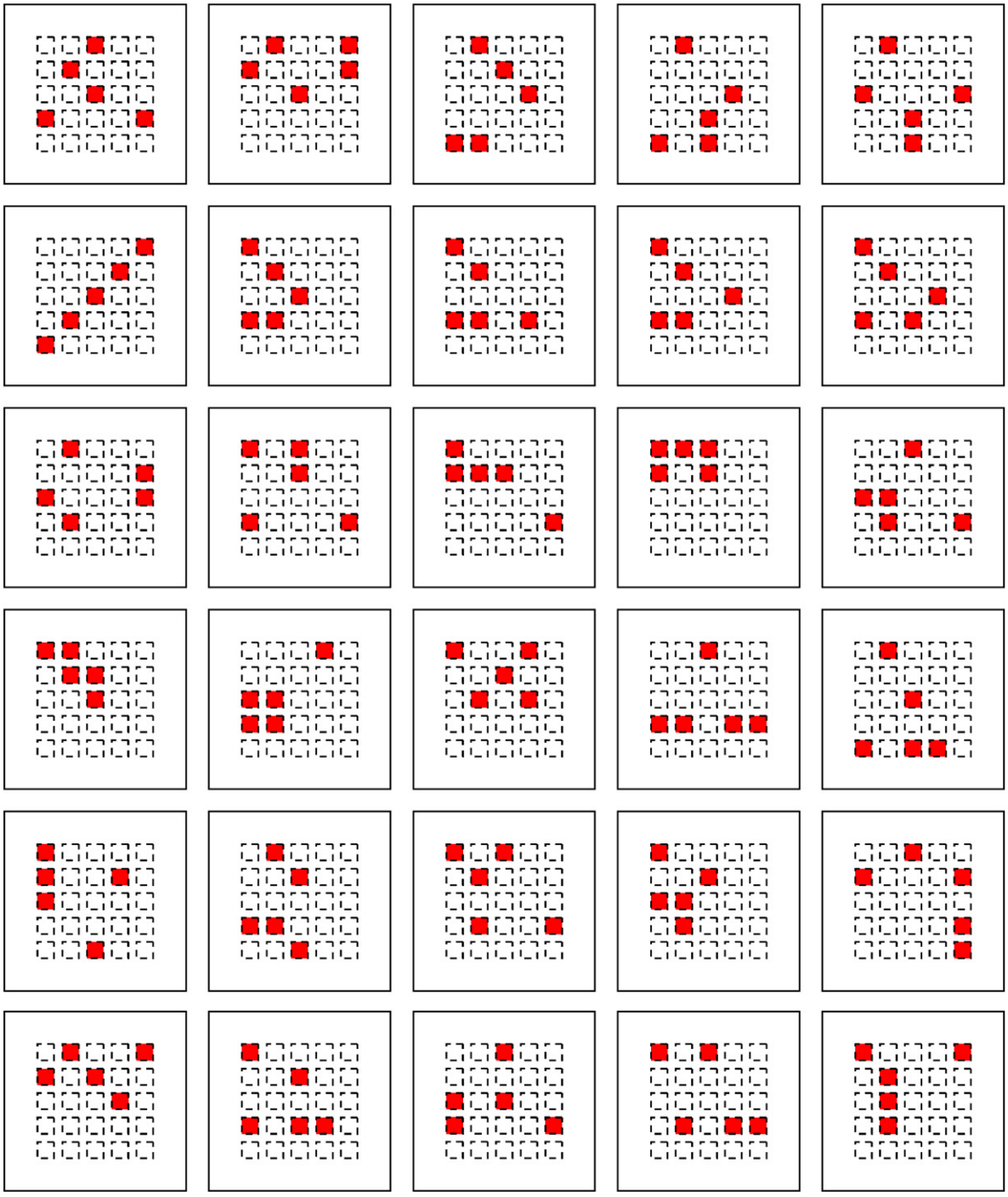

Fig. 11. Diagram showing the position of heat sources used for predicting the temperatures by the trained network.

the absolute temperatures and compared with the temperatures from CFD simulations. Table 5 presents the maximum temperatures predicted by ANN and CFD and their difference. From Table 5, it is seen that the maximum relative error is within $\pm 5\%$.

Finally, the trained network is used to predict the temperature of five heat sources for all possible distinct configurations. The number of distinct configurations is ${}^{25}C_5$. The maximum temperatures in these cases are sorted in the descending order of their magnitude and are plotted along with their average temperatures, as shown in Fig. 12. The "best" configuration is the one that has the lowest maximum temperature and a relatively small temperature difference among five heat sources. The temperatures of the heat sources of the best configuration predicted by the ANN and the corresponding temperatures obtained from the numerical simulations are given along with the best configuration in Fig. 13. Many configurations are observed to have maximum temperatures that are very close to the temperatures encountered in the best configuration. These configurations can be treated as near optimum configurations, which are not easily

Table 5
Comparison of maximum temperatures predicted by ANN with CFD

S. No	Position of heat sources	Maximum temperature (°C)		% error
		ANN	CFD	
1	41-22-13-33-45	112.5	112.7	0.12
2	21-12-33-15-25	118.6	121.3	2.17
3	51-12-52-23-34	106.6	105.9	0.75
4	51-12-43-53-34	122.2	121.4	0.65
5	31-12-23-14-35	93.5	93.4	0.10
6	51-42-33-24-15	94.0	93.4	0.56
7	11-41-22-42-33	112.0	112.0	0.02
9	11-41-22-42-44	112.6	111.5	1.00
10	11-41-22-42-34	113.1	111.6	1.29
11	11-41-22-42-34	108.1	108.3	0.16
12	31-12-42-25-35	120.6	121.3	0.55
13	11-41-13-23-45	121.6	121.4	0.12
14	11-21-22-23-33	125.9	120.0	4.91
15	11-21-12-13-23	123.6	120.0	2.99
16	31-32-42-13-45	121.1	120.9	0.17
17	11-12-22-23-33	122.2	121.1	0.90
28	31-41-32-42-14	120.4	121.1	0.56
19	11-32-23-14-34	112.0	111.3	0.62
20	41-42-13-33-24	111.6	112.2	0.51
21	51-12-33-53-54	113.1	110.9	1.94
21	11-21-31-53-24	136.0	139.1	2.21
22	41-12-42-23-53	111.0	108.8	1.99
23	11-22-42-13-45	113.0	114.6	1.42
24	11-31-32-42-23	122.1	121.8	0.30
25	21-13-25-45-55	140.2	136.3	2.88
26	11-22-32-42-15	133.8	139.5	4.04
27	21-12-23-34-15	93.1	93.4	0.39
28	11-41-23-43-44	113.1	110.9	1.98
29	31-41-13-33-45	127.7	121.1	5.46
30	11-42-13-44-45	93.2	93.8	0.59

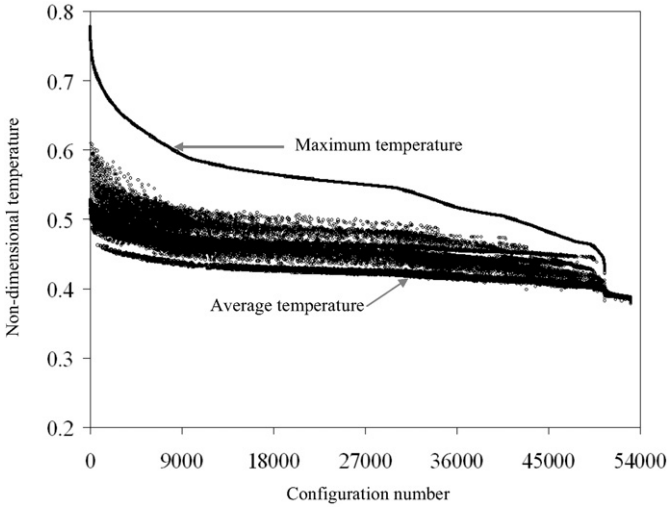

Fig. 12. Maximum and average temperatures of heat sources of all possible configurations.

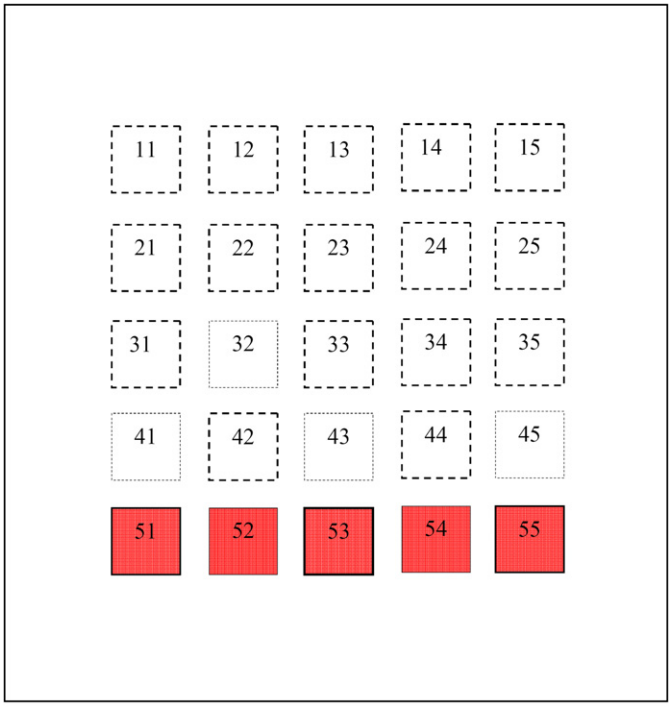

	Temperature, °C				
	51	52	53	54	55
ANN	92.1	91.5	91.0	90.9	89.9
CFD	90.1	90.5	90.3	90.5	90.1

Fig. 13. Best possible position predicted by ANN.

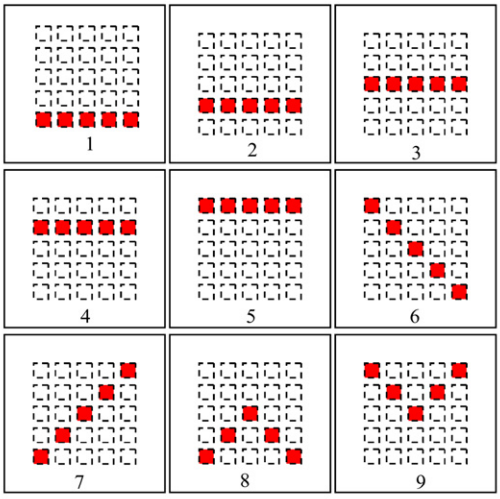

Maximum temperature , ^{0}C									
Case	1	2	3	4	5	6	7	8	9
ANN	92.1	93.1	93.4	93.9	94.3	93.1	93.9	92.9	92.9
CFD	90.5	90.5	90.5	90.5	90.5	95.0	95.0	93.4	93.3

Fig. 14. Near optimum configurations predicted by ANN.

determined by other search methods. The near optimum configurations are shown in Fig. 14, along with their maximum temperatures.

From Fig. 14, it can be observed that those configurations, in which the heat sources are placed one in each column regardless of the row number, have maximum temperatures very close to the temperature of the best configuration. This is because of low thermal interaction in the lateral direction as there is sufficient gap between the adjacent heat sources. However, the temperature of the heat source located down stream of the flow is slightly above the temperature of the heat source located in the upstream side due the growth in the boundary layer. In

configurations where one or more heat sources are placed back to back in a particular column, regardless of the row number the temperature of the heat source on the down stream side is strongly affected by the heat source placed upstream because of the effect of the boundary layer growth. The worst configuration is one in which all five heat sources are placed in a single column.

Thus, by the use of ANN we are not only in a position to capture the complex physics in the problem, but are able to perform an exhaustive search, considered either as a luxury or impossibility in many multi-parameter problems. As the total number of combinations was fixed in the present study, an exhaustive search was possible and eventually the optimal configuration was determined. Hence by the use of ANN, one is in a position to have a "fast" model that holds the key to optimization. Even in those problems, where an exhaustive search is prohibitively expensive, ANN can be used to drive a data driven optimization technique like Genetic Algorithms or Bayesian inference. Such a hybrid approach opens up new vistas in optimization involving complex fluid flow and heat transfer.

5. Conclusions

For three-dimensional laminar mixed convection in a vertical duct, with 5 discrete heat sources on one of the walls, limited "full" CFD solutions were used to train an artificial neural network (ANN) to predict the maximum temperature of the discrete heat sources. The trained neural network was tested with data that were not used for the training and the by ANN predictions agree reasonably well with the data obtained by numerical simulations. A few numerical simulations (less than 1%) were used in the training and testing phases of neural network for the present analysis to predict the temperatures of the heat sources of all possible configurations. Based on an exhaustive search, the best configuration was determined from amongst the candidate configurations for the lowest maximum temperature. For this problem, it is seen that there are several "near" optimal solutions. An attempt has thus been made to establish the feasibility of using ANN for obtaining an optimal system in multi parameter problems involving both fluid flow and heat transfer, where the functional relationship is exceedingly complex or not known.

References

[1] A.K. da Silva, S. Lorente, A. Bejan, Optimal distribution of discrete heat sources on a plate with laminar forced convection, International Journal of Heat and Mass Transfer 47 (2004) 2139–2148.
[2] A.K. da Silva, S. Lorente, A. Bejan, Optimal distribution of discrete heat sources on a wall with laminar natural convection, International Journal of Heat and Mass Transfer 47 (2004) 203–214.
[3] A.K. da Silva, G. Lorenzini, A. Bejan, Distribution of heat sources in vertical open channels with natural convection, International Journal of Heat and Mass Transfer 48 (2005) 1462–1469.
[4] T. Dias, L.F. Milanez, Optimal location of heat sources on a vertical wall with natural convection through genetic algorithms, International Journal of Heat and Mass Transfer 49 (2006) 2090–2096.
[5] Y. Liu, N. Phan-Thien, An optimum spacing program for three chips mounted on a vertical substrate in an enclosure, Numerical Heat Transfer, Part A 37 (2000) 613–630.
[6] S. Chen, Y. Liu, An optimum spacing problem for three-by-three heated elements mounted on a substrate, Heat and Mass Transfer 29 (2002) 3–9.
[7] N. Queipo, R. Devarakonda, A.C.J. Humphery, Genetic algorithms for thermosciences research: application to the optimized cooling of electronic components, International Journal of Heat and Mass Transfer 37 (1994) 893–908.
[8] M. Rajeev Reddy, C. Balaji, Optimization of the location of multiple discrete heat sources in a ventilated cavity using artificial neural networks and micro genetic algorithm, International Journal of Heat and Mass Transfer 51 (2007) 2299–2312.
[9] S.S. Sablani, A. Kacimove, J. Perret, A.S. Mujumdar, A. Campo, Non-iterative estimation of heat transfer coefficients using artificial neural network models, International Journal of Heat and Mass Transfer 48 (2005) 665–679.
[10] M.A. Mahmoud, A.E. Ben-Nakhi, Neural networks analysis of free laminar convection in a partitioned enclosure, Communications in Nonlinear Science and Numerical Simulation 12 (2007) 1265–1276.
[11] J. Thibault, B.P.A. Grandjean, A neural network methodology for heat transfer data analysis, International Journal of Heat and Mass Transfer 34 (1991) 2063–2070.
[12] J.Z. Gregory, M.C. Louay, K.D. Walters, Correlating heat transfer and friction in helically-finned tubes using artificial neural networks, International Journal of Heat and Mass Transfer 50 (2007) 4713–4723.
[13] Y. Islamoglu, A. Kurt, Heat transfer analysis using ANNs with experimental data for air flowing in corrugated channels, International Journal of Heat and Mass Transfer 47 (2004) 1361–1365.
[14] A.T. Joseph, S.P. Venkateshan, G. Kuruvilla, Experimental studies on cooling of electronic components in a channel, International Journal of Transport Phenomena 3 (2001) 103–118.
[15] F.M. Ham, I. Kostanic, Principles of Neurocomputing for Science and Engineering, third ed., Tata McGraw-Hill Publishing Company Limited, New Delhi, 2006.